Performance Analysis of RF Energy Harvesting and Information Transmission based on NOMA with Interfering Signal for IoT Relay Systems

Ashish Rauniyar, *Student Member, IEEE,* Paal Engelstad, *Senior Member, IEEE,* and Olav N. Østerbø, *Senior Member, IEEE*

***Abstract*—Owing to the exponential proliferation of the Internet of Things (IoT), it is anticipated that the number of small IoT devices will grow expeditiously over the next few years. These billions of small IoT sensor and devices will consume a huge power for data transmission. In this fashion, Radio frequency (RF) energy harvesting has been contemplated as an appealing solution to the architecture of long-term and self-sustainable next-generation wireless systems such as IoT network. However, in the practical environment, such IoT network or systems are subjected to external interference factors which often results in the loss of the system rate. Different from generic RF EH system in the literature where only a source node data is relayed through intermediate EH relaying node, in this paper, we have considered to transmit the data of IoT relay node along with source node data using Non-orthogonal multiple access (NOMA) protocol in the presence of an interfering signal to their respective destinations. Specifically, in the presence on interfering signal, we study the combination of two popular energy harvesting relaying architectures-time switching (TS) relaying and power splitting (PS) relaying with NOMA protocol for IoT relay systems. Considering the interference from the external entity, we have mathematically derived the outage probability, throughput and sum-throughput for our proposed system. Extensive simulations are carried out to find out the optimal TS and PS factor that maximizes the sum-throughput of the considered system in the presence of an interfering signal. The analytical results of our system model under consideration are validated by the simulation results, and representative performance comparisons are presented.**

***Index Terms*—Radio frequency, Internet of Things, NOMA, energy harvesting, relaying, interference, time switching, power splitting, outage probability, throughput, sum-throughput, optimization.**

I. Introduction

CISCO has anticipated that there will be 50 billion of small sensors or Internet of Thing (IoT) devices connected to the Internet by 2020 [1]. Alongside the exponential proliferation of the IoT, the forthcoming fifth generation (5G) network is capable of interconnecting heterogeneous IoT sensor or devices for effective device-to-device (D2D), machine-to-machine (M2M) communications as well as facilitating various IoT services and applications [2][3][4]. Due to the technological development in IoT, automation is fully possible without any human intervention [5]. The core of distributed automation by these IoT sensor and devices is essentially the reliable exchange of data and information among them [6]. Data transmission and communication amidst these small sensors and IoT devices will consume an enormous amount of power. However, it is to be noted that these small IoT sensors or devices are usually battery powered. Essentially, energy is a limited resource of eminent importance as much longer operation lifetime is expected in the next generation wireless networks such as IoT networks for self-sustainable green communications [7]. Energy efficient data transmission is a viable solution to extend the lifetime of these resource constrained sensors nodes in the context of IoT.

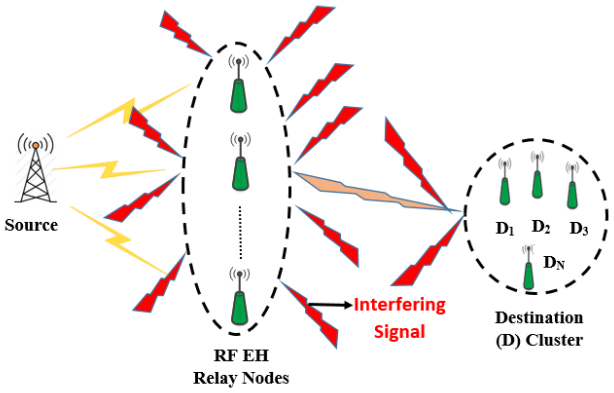

Fig. 1. Generic RF EH relay communication system with interfering signals

However, in the practical environment, such IoT network or systems are subjected to the external interference factors which often results in the loss of the system rate [8]. Moreover, cooperative communication has been widely considered to combat wireless impairments such as fading and other environmental factors [9], [10], [11], [12]. However, the cooperation for relaying the information comes at extra energy consumption of the relay node that may prevent the battery operated IoT nodes or devices to take an efficacious part in relaying. Recently, energy harvesting (EH) from radio frequency (RF) signals have emerged as a promising candidate to fulfil the energy requirements of the massive IoT sensor and devices [13][14]. The IoT sensor or devices can be recharged through EH mechanism by the directed RF signal from the source node

A. Rauniyar and P. Engelstad is with the Autonomous Systems and Sensor Technologies Research Group, Department of Technology Systems, University of Oslo, Oslo, 0316, Norway and Autonomous System and Network (ASN) Research Group, Department of Computer Science, Oslo Metropolitan University, Oslo, 0130, Norway (e-mail: ashish@oslomet.no;paalen@oslomet.no).

O. N. Østerbø is with Telenor Research, Oslo, 1360, Norway (e-mail: olav.osterbo@getmail.no).

[15]. In [16], it is shown that to charge a 5V super-capacitor utilizing RF wireless EH technology, their proposed system was able to work with a minimum input power of -10 dBm (0.1 mW). Further, the authors in [17] demonstrated that the wireless sensor node received 3.14 mW of power through the air at a distance of $1m$ from $3W$ source by RF EH. This amount of power is sufficient for the operation of the sensors nodes which indicates the usefulness of RF EH in wireless sensor network [18].

Since RF signal carries both energy and information simultaneously, the IoT sensor or nodes can recharge themselves through RF EH and at the same time decode the information data and then relay or transmits the information of the source node to its destination [19]. Due to practical consideration, simultaneous information and power transfer (SWIPT) is not feasible as EH circuitry is not able to harvests the energy and decode the information from the source node RF signal at the same time [20]. Therefore, time switching (TS) relaying and power splitting relaying (PS) are the two popular EH architecture widely considered in the literature for EH and information processing separately [21]. In TS relaying, the receiver alternatively switches between the energy harvesting mode and information decoding mode over time. In PS relaying, the receiver splits the incoming signal into two part; one part is used for EH and another part is used for information decoding. Since, we have employed TS and PS relaying in our system model, the working of TS and PS relaying is explained in the next section. Meanwhile, non-orthogonal multiple access (NOMA) has been proposed as an essential enabling technology for the next generation networks such as 5G networks and beyond to meet the heterogeneous demands of such networks and thereby providing spectral efficiency and capacity gain [22][23][24]. Different from conventional orthogonal multiple access schemes, the principal concept of NOMA is to assist multiple users with different power levels in the same frequency band [25]. More precisely, to achieve a balanced trade-off between system throughput and user fairness, users with worse channel conditions are allocated with more transmit power and users with better channel conditions are allocated less transmitting power in power domain NOMA. Therefore, by using successive interference cancellation (SIC) at the receiver side, users can be separated [26].

An illustration of generic RF EH relay communication systems with interfering signals is shown in Fig. 1 where a source node selects one of the best RF EH relay to transmit its information to its intended destination. The network is subjected to the interfering signals from the external entity which affects the system performance. To the best of author's knowledge, most of the related literature in this domain is confined to cooperatively transmitting the source node data by EH relay node to the destination node. In this paper, we have also considered transmitting the data of the relay node that may be an IoT sensor node in the context of IoT which needs to transmit its own information along with the source node data by using NOMA protocol in the presence of interfering signal to their respective destinations. Specifically, we investigate the performance analysis of time switching relaying and power splitting relaying with NOMA protocol for IoT relay systems with interfering signal.

Considering the practical application of our proposed system model, it can be used in coal mines, tunnels, underground train, hazardous environments like nuclear reactors and toxic environments where a number of sensors and IoT devices are employed such as indicators, detectors, alarms etc. for effective operation. In such areas, it is staggeringly difficult to manually replace the battery of sensor nodes or IoT devices and connect all of them through wired connections. Thus, by employing RF EH, it is convenient to recharge the wireless IoT sensor nodes. Further, by exploiting NOMA technology, multiple IoT users data can be transmitted together and thereby enhancing the spectral efficiency and capacity demands in such environments. In addition, due to the involvement of numerous IoT sensors and technologies in those areas, interference from an external entity is inevitable. Thus, it is crucial to do the performance evaluation of a deployed system when an interference constraint is considered in such environments. Considering all these situations in hand, we think that our considered system model can be applicable in those above-mentioned areas.

A wireless powered amplify-and-forward (AF) and decode-and-forward (DF) time switching relaying for cooperative EH based communication was investigated in [27]. The authors derived the analytical expressions for the achievable throughput. However, no practical interference constraint was considered for their model. An interference aided energy harvesting model was proposed for cooperative relaying systems in [28]. The author studied the TS and PS relaying scheme where the relay harvests the energy from the source RF signal and co-channel interference and then transmit the information to the destination node. The authors investigated their scheme on three terminal model namely source-relay-destination. The authors in [29] studied three relaying protocols, the time switching relaying (TSR) protocol, the power splitting relaying (PSR) protocol and hybrid TSR-PSR protocol in the presence of an interfering signal. The authors derived the analytical expressions for the outage probability and throughput in the delay-sensitive transmission mode for the aforementioned three protocols. However, the investigated model was limited to three terminal model-source-relay-destination with the interfering signal. The authors in [30] investigated the performance of dual-hop AF relaying networks under the impact of co-channel interference at the two source nodes and the EH relay. The authors derived the closed-form expressions for outage probability and bit error ratio (BER) to analyze the system performance. There has also been NOMA based EH study. The authors in [31] proposed EH protocol based on time power switching-based relaying (TPSR) architecture for AF mode where the EH-NOMA based relay helps the source node which transmits two symbols for the two destination node. However, no interference constrain was considered or investigated in their model. Different from most of the related works in this domain, in our earlier work [32], we proposed and investigated RF energy harvesting and information transmission based on NOMA for Wireless Powered IoT relay systems where a source node information data is relayed through power constrained IoT relay node IoT_R that first harvests the energy

from source node RF signal using either TS and PS relaying protocol and then transmits the source node information along with its information using NOMA protocol to the respective destination nodes. But no interference constraint was considered in our previous work. In this paper, we extend our previous work in [32] by introducing the interfering signal in our system model and investigating the performance analysis of RF EH and information transmission based on TS, PS and NOMA for IoT relay systems. Furthermore, we derived the closed-form analytical expressions for the outage probability, throughput, and sum-throughput for our system model under consideration with the interfering signal.

Securing the communication is a challenging problem to be solved and can affect RF communication to a great extent in IoT relay systems. The open nature of the wireless medium enables unauthorized nodes to eavesdrop on the communication between any two legitimate nodes. Traditionally, secure communication can be achieved through upper-layer cryptographic methods that involve intensive key distributions which may not be suitable for resource and power constrained IoT relay systems. Wyner introduced the information theoretic approach ,i.e. secrecy rate to securely transmit the confidential messages without using an encryption key to a legitimate receiving node by exploiting the inherent randomness of the physical medium [33]. Investigating secrecy capacity for secured communication in IoT relay systems is an interesting topic of our future work.

In summary, the major contribution of this paper can be outlined as:

- Considering the practical interference constraint and realizing the energy constrained nature of IoT nodes, we have considered and investigated an RF EH-based on TS, PS and NOMA with interfering signal for IoT relay systems.
- Different from generic RF EH system in the literature where only a source node data is relayed through intermediate EH relaying node, in this paper, we have also considered transmitting the data of IoT relay node along with the source node data using NOMA protocol in the presence of interfering signal to their respective destinations. Specifically, we study the combination of two popular energy harvesting relaying architectures-time switching relaying and and power splitting relaying with NOMA protocol for IoT relay systems in the presence on interfering signal.
- We have mathematically derived the outage probability, throughput and sum-throughput for our considered scenario.
- Our proposed system analytical results for TS, PS relaying and NOMA with interfering signal are validated by simulation results. The developed analysis is corroborated through Monte-Carlo simulations and some representative performance comparisons are presented.

The rest of the paper is organized as follows. In Section II, we present our system model. In Section III, we explain our channel model. Section IV deals with the considered system model based on time switching and NOMA protocol with interfering signal along with outage probability, throughput

TABLE I
ABBREVIATIONS AND CORRESPONDING SYMBOLS

Symbol	Meaning
IoT_R	IoT relay node
P_s	Power of source node transmit signal
P_I	Power of interfering signal
P_{I,IoT_R}	Interference power at IoT_R
$P_{I,s_{rec}}$	Interference power at source user destination node
$P_{I,IoT_{rec}}$	Interference power at IoT user destination node
$F_\gamma(x)$	Cumulative distributive function (CDF)
$f_\gamma(x)$	Probability distributive function (PDF)
RV	Random variable
RF	Radio Frequency
EH	Energy Harvesting
SNR	Signal-to-noise ratio
NOMA	Non-orthogonal multiple access
TS	Time switching
PS	Power splitting
DF	Decode and Forward
ε	Power splitting factor
x_s	Source node information data
T	Time period
y_{IoT_R}	Information signal received at IoT_R
n_{IoT_R}	Additive White Gaussian Nosie at IoT_R
$\sigma^2_{IoT_R}$	Noise variance at IoT_R
h	Channel co-efficient between source node and IoT_R node
λ_h	Mean variance of h
g	Channel co-efficient between IoT_R and source user destination node
λ_g	Mean variance of g
z	Channel co-efficient between IoT_R and IoT user destination node
λ_z	Mean variance of z
f_1	Channel co-efficient between interferer and IoT_R
λ_{f_1}	Mean variance of f_1
f_2	Channel co-efficient between interferer and source user destination node
λ_{f_2}	Mean variance of f_2
f_3	Channel co-efficient between interferer and IoT user destination node
λ_{f_3}	Mean variance of f_3
η	Energy conversion efficiency
$E_{H_{IoT_R}}$	Energy harvested at IoT_R node
P_{IoT_R}	Transmit power of IoT_R node
$Z_{I_{C1}}$	Superimposed composite signal for NOMA protocol
ϕ_1,ϕ_2	Power allocation factors for NOMA protocol
x_{IoT_R}	IoT_R node information data
$y_{s_{rec}}$	Received signal at source user destination node
$y_{IoT_{rec}}$	Received signal at IoT user destination node
$n_{s_{rec}}$	Additive White Gaussian Nosie at source user destination node
$n_{IoT_{rec}}$	Additive White Gaussian Nosie at IoT user destination node
γ_{IIoT_R}	Received SNR at IoT_R node
δ	Transmit SNR
$\gamma_{I_{s_{rec}}}^{x_{IoT_R}\rightarrow x_s}$	SNR required at the source user destination node to decode and cancel IoT_R information data
$\gamma_{Is_{rec}}$	Received SNR at the source user destination node
$\gamma_{IIoT_{rec}}$	Received SNR at IoT_R user destination node
$\sigma^2_{s_{rec}}$	Noise variance at source user destination node
$\sigma^2_{IoT_{rec}}$	Noise variance at IoT_R user destination node
ψ	Outage probability
P_{IOut_S}	Outage probability of source user node
$P_{IOut_{IoT_R}}$	Outage probability of IoT_R user node
$P_{Exact-IOut_{IoT_R}}$	Exact outage probability of IoT_R user node
R	Rate in bits per second per hertz
Thr_{IS}	Throughput of source user node
Thr_{IIoT_R}	Throughput of IoT_R user node
$Thr_{Exact-IIoT_R}$	Exact throughput of IoT_R user node
Thr_I	Sum-throughput of whole system
α^*	Optimal time switching factor
$K_1(.)$	First-order modified Bessel function of the second kind
$E_n(a)$	Exponential integral of order n

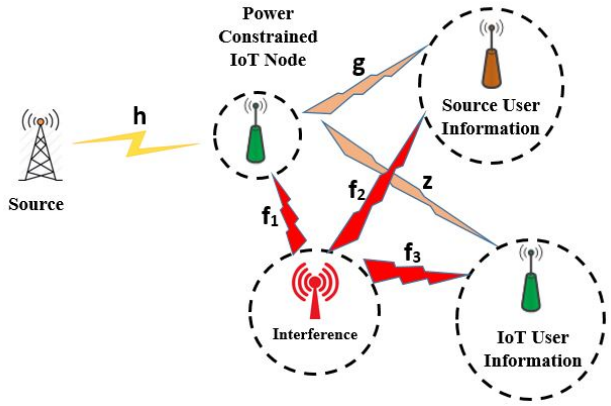

Fig. 2. Considered system model scenario with interfering signal

and sum-throughput derivations. Section V deals with the considered system model based on power splitting and NOMA protocol with interfering signal along with outage probability, throughput and sum-throughput derivations. In Section VI, we explain the algorithm - Golden section search method to find out the optimal time switching and power splitting factor that maximizes the sum-throughput for our considered scenario. Numerical results and discussions are presented in Section VII. Conclusion and future works are drawn in Section VIII.

II. System Model

We have considered a scenario as shown in Fig. 2, where a source has to transmit its information data to the destination i.e. source user information destination in the presence of an interfering signal from the external source or entity. It is assumed that there are no direct links between the source user node due to deep shadowing or blockage; thus information exchange between them only relies on the relay IoT_R. Therefore, it requires the help of the IoT node (IoT_R) for relaying its information data to its intended destination. IoT_R is rather power constrained node that acts as a DF relay and it will first harvest RF energy from the source signal using the time switching relaying or power splitting relaying protocol in the first stage and then transmits source information data along with its own data using NOMA protocol in the next stage. Here, IoT_R harvests the energy which is used for both source user and IoT_R data transmission to its respective destinations. The destination pair for source and IoT_R node serves as the receiving end for data transmission. Also, in the considered system, the network is subjected to the interference from the external entity or source (marked as red in Fig.2) which affects the system performance.

III. Channel Model

We have assumed that channel state information is perfectly known to the receiver and each of the nodes is equipped with a single antenna. Also, the nodes are assumed to be operating in the half-duplex mode. The channel between any two nodes is subjected to the independent Rayleigh block fading plus additive white Gaussian noise in which the channel

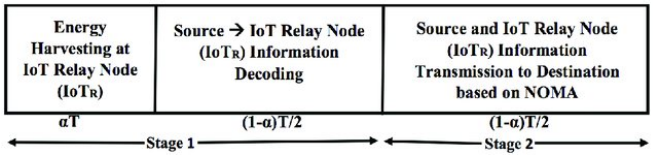

Fig. 3. Considered system model based on time switching (TS) and NOMA

remains constant during the transmission of a block and varies independently from one block to another. The reason for choosing a Rayleigh channel model is that it serves the purpose of modelling non-line-of-sight transmission. Rayleigh fading is viewed as a reasonable model for signal propagation as well as the effect of heavily built-up urban environments on radio signals [34]. Since, in our considered system model, we have assumed that there is no line-of-sight between the source user and its destination node due to deep fading or blockage, modelling the channel as Rayleigh channel model seems more reasonable. However, it is worth mentioning that when planning real networks, accurate models considering the specific situations are desirable, while for evaluation and experiments, simplified, idealized and generic models with few parameters are often preferable, and it is in line with most of the previous work in this domain such as [35][36]. Nevertheless, evaluating the performance of our system with other fading channel model is the interest of our future work.

Henceforth, $h \sim CN(0,\lambda_h)$ is the complex channel co-efficient between source node and IoT_R node with zero mean and variance λ_h. Similarly, $g \sim CN(0,\lambda_g)$ is the complex channel coefficient between IoT_R node and receiving source user destination node with zero mean and variance λ_g and $z \sim CN(0,\lambda_z)$ is the complex channel coefficient between IoT_R node and receiving IoT user destination node with zero mean and variance λ_z. Since, in the considered system, the network is subject to interference from the external entity, $f_i \sim CN(0,\lambda_{f_i})$ is the complex channel co-efficient between interferer and any node with zero mean and variance λ_{f_i}, where $i \in 1,2,3$ as shown in Fig.2. The link gain or channel gain is an exponential random variable (RV), whose cumulative distributive function (CDF) and probability density function (PDF) are given respectively as:

$$\begin{aligned} F_\gamma(x) &= 1 - e^{-\lambda_i x}, \\ f_\gamma(x) &= \lambda_i e^{-\lambda_i x}, \end{aligned} \tag{1}$$

where λ_i is the parameter of the channel gain between any two channels.

IV. Considered System Model based on Time Switching and NOMA with Interfering Signal

The system model under consideration based on TS and NOMA in the presence of an interfering signal is shown in Fig. 3. A basic time switching relaying protocol for energy harvesting and information processing at IoT_R is shown in Fig. 4. In this TS relaying scheme, power constrained IoT_R node first harvests the energy from source node's RF signal for αT duration and uses the time $\frac{(1-\alpha)T}{2}$ for information processing and $\frac{(1-\alpha)T}{2}$ for information transmission to source and IoT user

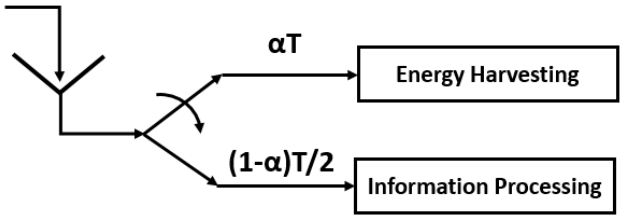

Fig. 4. Time switching protocol for energy harvesting and information processing at the IoT_R

using NOMA protocol. The network is subject to interference from some unknown source which affect the system performance. The detailed step of our proposed system model based on TS and NOMA with interfering signal is explained in the next sub-section. As shown in Fig. 2, the interference power from unknown source at the power constrained IoT relay node and the receiving source user destination node and IoT user destination node can be respectively given as:

$$P_{I,IoT_R} = P_I|f_1|^2 \tag{2}$$

$$P_{I,s_{rec}} = P_I|f_2|^2 \tag{3}$$

$$P_{I,IoT_{rec}} = P_I|f_3|^2 \tag{4}$$

where f_1, f_2,and f_3 are corresponding channel gains between the interfering transmitter and IoT relay node, receiving source user destination node and IoT user destination node respectively and P_I is the interference power of the interfering transmitter.

A. Stage 1

In this stage, the source transmits signal x_s with power P_s to the IoT_R for half of the block time T i.e., $T/2$ period of time. Here, IoT_R node works as TS based relay. The IoT_R node divide the time block in the ratio $\alpha T : \frac{(1-\alpha)T}{2} : \frac{(1-\alpha)T}{2}$ where αT is for energy harvesting by IoT_R and $\frac{(1-\alpha)T}{2}$ is for information processing by IoT_R respectively, $0 \leq \alpha \leq 1$. The information signal received at IoT_R during this stage is given as:

$$E_{H_{IoT_R}} = \eta P_s|h|^2\alpha T, \tag{5}$$

where $0 \leq \eta \leq 1$ is the energy conversion efficiency. The pre-processing power for the energy harvesting is assumed to be negligible in contrast to the transmission power P_{IoT_R} at IoT_R.

The transmit power of IoT_R i.e., P_{IoT_R} in $\frac{(1-\alpha)T}{2}$ block of time can be given as:

$$P_{IoT_R} = \frac{E_h}{(1-\alpha)T/2} = \frac{2\eta P_s|h|^2\alpha}{(1-\alpha)}, \tag{6}$$

B. Stage-2

In this stage, the IoT_R node transmits a superimposed composite signal $Z_{I_{C1}}$ which consists of source information x_s and IoT_R information x_{IoT_R} to the respective destination of source and IoT relay node using NOMA protocol. The superimposed composite signal $Z_{I_{C1}}$ following NOMA protocol can be given as:

$$Z_{I_{C1}} = \sqrt{\phi_1 P_{IoT_R}}x_s + \sqrt{\phi_2 P_{IoT_R}}x_{IoT_R} \tag{7}$$

where $\phi_1 + \phi_2 = 1$ and $\phi_2 = 1 - \phi_1$.
Now, the received signals at the receiver of Source user and IoT user can be respectively given as:

$$y_{s_{rec}} = \sqrt{P_{IoT_R}}gZ_{I_{C1}} + n_{s_{rec}}, \tag{8}$$

$$y_{IoT_{rec}} = \sqrt{P_{IoT_R}}zZ_{I_{C1}} + n_{IoT_{rec}}, \tag{9}$$

where $n_{s_{rec}}$ and $n_{IoT_{rec}}$ is the additive white Gaussian noise at the receiver of source and IoT user node respectively with mean zero and variance $\sigma^2_{s_{rec}}$ and $\sigma^2_{IoT_{rec}}$. We have assumed that $g > z$. Therefore, $\lambda_g > \lambda_z$ and $\phi_1 < \phi_2$.

C. Outage Probability, Throughput and Sum-throughput

The received signal to noise ratio (SNR) at the IoT_R in the presence of an interfer is given by:

$$\gamma_{IIoT_R} = \frac{P_s|h|^2}{P_I|f_1|^2\sigma^2_{IoT_R}} = \frac{\delta X}{P_I F_1} \tag{10}$$

where $\delta \triangleq \frac{P_s}{\sigma^2_{IoT_R}}$, $|h|^2 \sim X$ and $|f_1|^2 \sim F_1$.

Similarly, the received SNR with x_{IoT_R} and x_s at the receiving source user in the presence of interfer is given by:

$$\gamma^{x_{IoT_R}\to x_s}_{Is_{rec}} = \frac{\phi_2 P_{IoT_R}|g|^2}{\phi_1 P_{IoT_R}|g|^2 P_I|f_2|^2 + \sigma^2_{s_{rec}}} = \frac{\phi_2 P_{IoT_R} Y}{\phi_1 P_{IoT_R} Y P_I F_2 + 1} \tag{11}$$

$$\gamma_{Is_{rec}} = \frac{\phi_1 P_{IoT_R}|g|^2}{P_I|f_2|^2\sigma^2_{s_{rec}}} = \frac{\phi_1 P_{IoT_R} Y}{P_I F_2} \tag{12}$$

where $\gamma^{x_{IoT_R}\to x_s}_{Is_{rec}}$ is the SNR required at x_s to decode and cancel x_{IoT_R} and $|g|^2 \sim Y$ and $|f_2|^2 \sim F_2$ and $\sigma^2_{s_{rec}} = 1$.

The received SNR at IoT user associated with symbol x_{IoT_R} in the presence of interfering signal is given by:

$$\gamma_{IoT_{rec}} = \frac{\phi_2 P_{IoT_R}|z|^2}{\phi_1 P_{IoT_R}|z|^2 P_I|f_3|^2 + \sigma^2_{IoT_{rec}}} = \frac{\phi_2 P_{IoT_R} Z}{\phi_1 P_{IoT_R} Z P_I F_3 + 1} \tag{13}$$

where $|z|^2 \sim Z$ and $|f_3|^2 \sim F_3$ and $\sigma^2_{IoT_{rec}} = 1$.

As the data transmission is break down into two separate hops which are independent of each other. Hence, the outage occurs only if source to IoT_R path and IoT_R to corresponding destination path fails to satisfy the SNR constraint. Therefore, the outage probability of the source node in the presence of interfering signal can be given as:

$$P_{IOut_S} = Pr(min(\gamma_{IoT_R}, \gamma_{s_{rec}}) \leq \psi) \tag{14}$$

where $\psi = 2^R - 1$ is the lower threshold for SNR i.e., outage probability.
Similarly, the outage probability of the IoT relay node IoT_R in the presence of interfering signal can be given as:

$$P_{IOut_{IoT_R}} = Pr(min(\gamma^{x_{IoT_R}\to x_s}_{s_{rec}}, \gamma_{IoT_{rec}}) \leq \psi) \tag{15}$$

Hence, the throughput of the source node in the presence of interfering signal can be given as:

$$Thr_{IS} = \frac{(1 - P_{Iout_S})(1-\alpha)R}{2} \tag{16}$$

where R is the transmission rate in bits per second per hertz. The throughput of the IoT relay node IoT_R in the presence of interfering signal can be given as:

$$Thr_{IIoT_R} = \frac{(1-P_{IOut_{IoT_R}})(1-\alpha)R}{2} \tag{17}$$

Therefore, the sum-throughput of the whole system using TS and NOMA with interfering signal can be given as:

$$\begin{aligned} Thr_I &= Thr_{IS} + Thr_{IIoT_R} \\ &= \frac{(1-P_{IOut_S})(1-\alpha)R}{2} + \frac{(1-P_{IOut_{IoT_R}})(1-\alpha)R}{2} \end{aligned} \tag{18}$$

Theorem 1: The closed form expressions for outage probability and throughput of the source node using TS and NOMA with interfering signal can be expressed as:

$$P_{IOut_S} = \lambda_h m e^{\lambda_h m} Ei(m\lambda_h) - \lambda_h m e^{(n+\lambda_h)m} Ei\big((n+\lambda_h)m\big) + \frac{\lambda_h}{(n+\lambda_h)} \tag{19}$$

$$Thr_{IS} = \frac{(1-\alpha)R}{2}\left(1 - \lambda_h m e^{\lambda_h m} Ei(m\lambda_h) + \lambda_h m e^{(n+\lambda_h)m} Ei\big((n+\lambda_h)m\big) - \frac{\lambda_h}{(n+\lambda_h)}\right) \tag{20}$$

where $m = \frac{\lambda_g \psi}{\lambda_{f_2} b}$, $n = \frac{\lambda_{f_1} a}{\psi}$, $a = \frac{\delta}{P_I}$, $b = \frac{2\eta\phi_1 P_s \alpha}{(1-\alpha)P_I}$ and $Ei(.)$ is the exponential integral function.

Proof: The detailed proof is given in Appendix A.

Theorem 2: The closed form expressions for outage probability and throughput of the IoT relay node using TS and NOMA with interfering signal can be expressed as:

$$P_{IOut_{IoT_R}} = 1 - \sum_{i=0}^{\infty}\sum_{j=0}^{\infty} i!\,j!\,C_{ij}\left(\frac{b_2\psi}{a_2}\right)^i\left(\frac{b_3\psi}{a_3}\right)^j \times \left(1 - S_i\big(\frac{a_2}{b_2\psi}\big)e^{-\frac{a_2}{b_2\psi}}\right)\left(1 - S_j\big(\frac{a_3}{b_3\psi}\big)e^{-\frac{a_3}{b_3\psi}}\right) \tag{21}$$

$$Thr_{IIoT_R} = \frac{(1-\alpha)R}{2}\sum_{i=0}^{\infty}\sum_{j=0}^{\infty} i!\,j!\,C_{ij}\left(\frac{b_2\psi}{a_2}\right)^i\left(\frac{b_3\psi}{a_3}\right)^j \times \left(1 - S_i\big(\frac{a_2}{b_2\psi}\big)e^{-\frac{a_2}{b_2\psi}}\right)\left(1 - S_j\big(\frac{a_3}{b_3\psi}\big)e^{-\frac{a_3}{b_3\psi}}\right) \tag{22}$$

where $l = \frac{2\eta P_s \alpha}{(1-\alpha)}$, $t = \frac{2\eta P_s \alpha P_I}{(1-\alpha)}$, $a_2 = \frac{\lambda_{f_2}\lambda_h\lambda_g}{\phi_1 t}$, $a_3 = \frac{\lambda_{f_3}\lambda_h\lambda_z}{\phi_1 t}$, $b_2 = \frac{\lambda_h\lambda_g}{\phi_2 l}$, $b_3 = \frac{\lambda_h\lambda_z}{\phi_2 l}$, $C_{ij} = \sum_{l=0}^{i}\sum_{k=0}^{j}\frac{1}{k!\,l!}\binom{i-1}{l-1}\binom{j-1}{k-1}H^{(k+l)}(b_2\psi + b_3\psi)(b_2\psi)^l(b_3\psi)^k$, $H^{(n)}(z) = (-1)^n 2(\sqrt{z})^{1-n}K_{n-1}(2\sqrt{z})$ and $S_k(a) = \sum_{s=0}^{k}\frac{a^s}{s!}$ is truncated exponential series.

Proof: The detailed proof is given in Appendix B.

Further, it should be noted in Theorem 2, unlike Theorem 1, the closed form expressions for $P_{IOut_{IoT_R}}$ and Thr_{IIoT_R} as given by Equation 21 and Equation 22 respectively, it is hard to do calculation due to the involvement of the complex terms. Therefore, we approximate the expressions in Equation 21 and Equation 22 upto 20 terms and compare it with the exact expressions as given by Equation 23 and 24 and verify it with our Monte Carlo simulation results which is shown and explained in the numerical result and discussions section below.

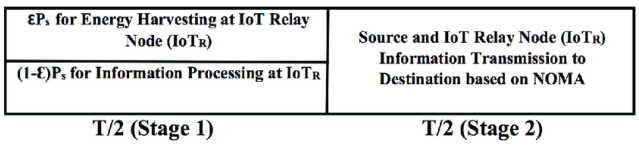

Fig. 5. Considered system model based on power splitting (PS) and NOMA

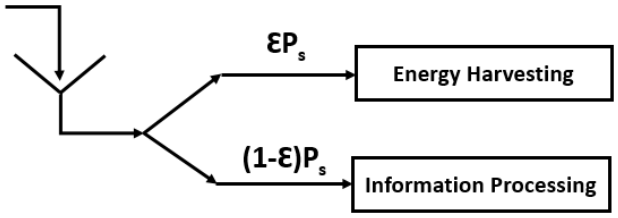

Fig. 6. Power splitting protocol for energy harvesting and information processing at the IoT_R

$$P_{Exact-IOut_{IoT_R}} = 1 - \lambda_{f_2}\lambda_{f_3}\int_0^{\frac{\phi_2 l}{\phi_1 t\psi}}\int_0^{\frac{\phi_2 l}{\phi_1 t\psi}} 2\sqrt{\frac{\lambda_h\lambda_g\psi}{\phi_2 l - \phi_1 t f_2\psi} + \frac{\lambda_h\lambda_z\psi}{\phi_2 l - \phi_1 t f_3\psi}} \times K_1\left(2\sqrt{\frac{\lambda_h\lambda_g\psi}{\phi_2 l - \phi_1 t f_2\psi} + \frac{\lambda_h\lambda_z\psi}{\phi_2 l - \phi_1 t f_3\psi}}\right)e^{-\lambda_{f_2} f_2}e^{-\lambda_{f_3} f_3}df_2 df_3 \tag{23}$$

$$Thr_{Exact-IIoT_R} = \frac{(1-\alpha)R\lambda_{f_2}\lambda_{f_3}}{2} \times \left(\int_0^{\frac{\phi_2 l}{\phi_1 t\psi}}\int_0^{\frac{\phi_2 l}{\phi_1 t\psi}} 2\sqrt{\frac{\lambda_h\lambda_g\psi}{\phi_2 l - \phi_1 t f_2\psi} + \frac{\lambda_h\lambda_z\psi}{\phi_2 l - \phi_1 t f_3\psi}} \times K_1\left(2\sqrt{\frac{\lambda_h\lambda_g\psi}{\phi_2 l - \phi_1 t f_2\psi} + \frac{\lambda_h\lambda_z\psi}{\phi_2 l - \phi_1 t f_3\psi}}\right)e^{-\lambda_{f_2} f_2}e^{-\lambda_{f_3} f_3}df_2 df_3\right) \tag{24}$$

Combining Equation 20 and Equation 22 gives the analytical expression for sum-throughput of the considered system using TS and NOMA with interfering signal. Similarly, combining Equation 20 and Equation 24 gives the analytical exact expression for sum-throughput of the considered system using TS and NOMA with interfering signal.

V. Considered System Model based on Power Splitting and NOMA with Interfering Signal

The system model under consideration based on PS and NOMA in the presence of an interfering signal is shown in Fig. 5. A basic power splitting relaying protocol for energy harvesting and information processing at IoT_R is shown in Fig. 6. In this PS relaying scheme, power constrained IoT_R node first harvests the energy from the source node signal

using εP_s where P_s is the power of the source node transmit signal. IoT_R uses remaining power $(1-\varepsilon)P_s$ for information processing. IoT_R transmits the respective information signal to source and IoT user destination node using NOMA protocol in $T/2$ period of time. As shown in Fig. 2, the network is subject to interference from some unknown source which affects the system performance. The detailed procedure of the considered system model based on PS and NOMA with interfering signal follows the same steps as TS and NOMA as explained in Section IV. The derivations of the outage probability, throughput and sum-throughput of the considered system based on PS and NOMA with interfering signal as given in Theorem 3 and Theorem 4, is straight forward which can be derived by following the same steps as in Appendix A and Appendix B. Due to page limitations, we have omitted the detailed explanation and derivations for the considered system based on PS and NOMA with interfering signal. We derived the final expressions for the outage probability and throughput of the source user and IoT_R user node for the considered system model based on PS and NOMA with interfering signal as shown in Theorem 3 and Theorem 4 respectively as:

Theorem 3: The closed form expressions for outage probability and throughput of the source node using PS and NOMA with interfering signal can be expressed as:

$$\hat{P}_{IOut_S} = \lambda_h c e^{\lambda_h c} Ei\big(c\lambda_h\big) - \lambda_h c e^{(d+\lambda_h)c} Ei\big((d+\lambda_h)c\big) + \frac{\lambda_h}{(d+\lambda_h)} \tag{25}$$

$$\hat{Thr}_{IS} = \frac{R}{2}\Bigg(1 - \lambda_h c e^{\lambda_h c} Ei\big(c\lambda_h\big) + \lambda_h c e^{(d+\lambda_h)c} Ei\big((d+\lambda_h)c\big) - \frac{\lambda_h}{(d+\lambda_h)}\Bigg) \tag{26}$$

where $c = \frac{\lambda_g \psi P_I}{\lambda_{f_2} \varepsilon \eta \phi_1 P_s}$ and $d = \frac{\lambda_{f_1}(1-\varepsilon)P_s}{P_I \psi}$ and $Ei(.)$ is the exponential integral function.

Theorem 4: The closed form expressions for outage probability and throughput of the IoT relay node using PS and NOMA with interfering signal can be expressed as:

$$\hat{P}_{IOut_{IoT_R}} = 1 - \sum_{i=0}^{\infty}\sum_{j=0}^{\infty} i!\,j!\,C_{ij}\left(\frac{r_2\psi}{q_2}\right)^i\left(\frac{r_3\psi}{q_3}\right)^j \times \left(1 - S_i\big(\frac{q_2}{r_2\psi}\big)e^{-\frac{q_2}{r_2\psi}}\right)\left(1 - S_j\big(\frac{q_3}{r_3\psi}\big)e^{-\frac{q_3}{r_3\psi}}\right) \tag{27}$$

$$\hat{Thr}_{IIoT_R} = \frac{R}{2}\sum_{i=0}^{\infty}\sum_{j=0}^{\infty} i!\,j!\,C_{ij}\left(\frac{r_2\psi}{q_2}\right)^i\left(\frac{r_3\psi}{q_3}\right)^j \times \left(1 - S_i\big(\frac{q_2}{r_2\psi}\big)e^{-\frac{q_2}{r_2\psi}}\right)\left(1 - S_j\big(\frac{q_3}{r_3\psi}\big)e^{-\frac{q_3}{r_3\psi}}\right) \tag{28}$$

where $o = \varepsilon\eta P_s$, $p = \varepsilon\eta P_s P_I$, $q_2 = \frac{\lambda_{f_2}\lambda_h\lambda_g}{\phi_1 p}$, $q_3 = \frac{\lambda_{f_3}\lambda_h\lambda_z}{\phi_1 p}$, $r_2 = \frac{\lambda_h\lambda_g}{\phi_2 o}$, $r_3 = \frac{\lambda_h\lambda_z}{\phi_2 o}$, $C_{ij} = \sum_{l=0}^{i}\sum_{k=0}^{j}\frac{1}{k!\,l!}\binom{i-1}{l-1}\binom{j-1}{k-1}H^{(k+l)}(r_2\psi + r_3\psi)(r_2\psi)^l(r_3\psi)^k$, $H^{(n)}(z) = (-1)^n 2(\sqrt{z})^{1-n}K_{n-1}(2\sqrt{z})$ and $S_k(a) = \sum_{s=0}^{k}\frac{a^s}{s!}$ is truncated exponential series.

The exact equation for outage probability and throughput of the IoT relay node can be given respectively as:

$$\hat{P}_{Exact-IOut_{IoT_R}} = 1 - \lambda_{f_2}\lambda_{f_3}\int_0^{\frac{\phi_2 o}{\phi_1 p\psi}}\int_0^{\frac{\phi_2 o}{\phi_1 p\psi}} 2\sqrt{\frac{\lambda_h\lambda_g\psi}{\phi_2 o - \phi_1 p f_2\psi} + \frac{\lambda_h\lambda_z\psi}{\phi_2 o - \phi_1 p f_3\psi}}\times K_1\left(2\sqrt{\frac{\lambda_h\lambda_g\psi}{\phi_2 o - \phi_1 p f_2\psi} + \frac{\lambda_h\lambda_z\psi}{\phi_2 o - \phi_1 p f_3\psi}}\right)e^{-\lambda_{f_2}f_2}e^{-\lambda_{f_3}f_3}df_2df_3 \tag{29}$$

$$\hat{Thr}_{Exact-IIoT_R} = \frac{R\lambda_{f_2}\lambda_{f_3}}{2}\times \left(\int_0^{\frac{\phi_2 o}{\phi_1 p\psi}}\int_0^{\frac{\phi_2 o}{\phi_1 p\psi}} 2\sqrt{\frac{\lambda_h\lambda_g\psi}{\phi_2 o - \phi_1 p f_2\psi} + \frac{\lambda_h\lambda_z\psi}{\phi_2 o - \phi_1 p f_3\psi}}\times K_1\left(2\sqrt{\frac{\lambda_h\lambda_g\psi}{\phi_2 o - \phi_1 p f_2\psi} + \frac{\lambda_h\lambda_z\psi}{\phi_2 o - \phi_1 p f_3\psi}}\right)e^{-\lambda_{f_2}f_2}e^{-\lambda_{f_3}f_3}df_2df_3\right) \tag{30}$$

VI. Sum-Throughput Maximization in the Presence of Interfering Signal

In order to maximize the sum-throughput for our system model under consideration based on TS, PS and NOMA in the presence of interfering signal, we need to find out optimal time switching factor α^* and optimal power splitting factor ε^* that gives the optimum performance for our model. It should be noted that, in practice, we cannot have higher a value for time switching factor α as although more energy can be harvested by having a higher α value, there will be less time allocated for the information processing. Hence, there will be an outage in the system. Similarly, we cannot have higher value for power splitting factor ε as although more energy can be harvested by having higher ε value, there will be less power allocated for the information processing which in turn will create an outage in the system. Therefore, finding optimum α^* and ε^* is important that can maximize the sum-throughput for our system model in the presence of interfering signal.

For sum-throughput maximization, we evaluate $\big(\frac{d\hat{Thr}(\alpha)}{d\alpha}\big)_{TS} = 0$ and $\big(\frac{d\hat{Thr}(\varepsilon)}{d\varepsilon}\big)_{PS} = 0$, where $Thr(\alpha)$ is the sum-throughput function with respect to time switching factor α and $\hat{Thr}(\varepsilon)$ is the sum-throughput function with respect to power splitting factor ε respectively. By thoroughly investigating the sum-throughput function for source and IoT node versus α and ε as shown in Fig. 13 and Fig. 14, we conclude that this is a concave function which has a unique maxima α^*, ε^* on the interval $[0,1]$ that maximizes the sum-throughput for our system model under consideration in the presence of interfering signal. Because of the involvement of the complex terms in the sum-throughput equation, the optimal α^* and ε^* can be computed through iterative numerical methods such as the Golden section search method. The detail working of the Golden section search method is explained in [32].

TABLE II
SIMULATION PARAMETERS

Parameter	Symbol	Values
Mean of $\|h\|^2 \to X$	λ_h	1
Mean of $\|g\|^2 \to Y$	λ_g	1
Mean of $z\|^2 \to Z$	λ_z	0.5
Mean of $\|f_1\|^2 \to F_1$	λ_{f_1}	1
Mean of $\|f_2\|^2 \to F_2$	λ_{f_2}	1
Mean of $\|f_3\|^2 \to F_3$	λ_{f_3}	1
Interference Threshold	P_I	5 dB
Source Node Transmit SNR	δ	0-20 dB
Energy Harvesting Efficiency	η	1
Source and IoT Node Rate	R	1bps/Hz
Power Factor for NOMA	ϕ_1	0.2
Power Factor for NOMA	ϕ_2	0.8

VII. NUMERICAL RESULTS AND DISCUSSIONS

In this section, we present Monte-Carlo simulation results to verify our analysis for our system model under consideration based on TS, PS and NOMA in the presence of interfering signal as explained in the previous section. For all the simulation, we have used the simulation parameters listed in Table I unless otherwise stated. We have used MATLAB to run the Monte-Carlo simulation by averaging over 10^5 random realizations of Rayleigh block fading channels h, g, z, f_1, f_2, f_3 to get the simulation results. In all the simulation figures in this section, $'TS_ISim'$, $'TS_IExa'$ and $'TS_IApp'$ represents Monte-Carlo simulation, analytical exact expression and analytical approximation respectively for our system model under consideration based on TS and NOMA in the presence of interfering signal. Similarly, $'PS_ISim'$, $'PS_IExa'$ and $'PS_IApp'$ represents Monte-Carlo simulation, analytical exact expression and analytical approximation respectively for our system model under consideration based on PS and NOMA in the presence of interfering signal.

In Fig. 7, the outage probability of the source user is plotted against the transmit SNR at different time switching factor α = 0.3, 0.5, & 0.7 and at different power splitting factor ε = 0.3, 0.5, & 0.7. As expected, the outage probability of the source user decreases with respect to increase in transmit SNR, α and ε for TS and PS relaying respectively in the presence of interfering signal. Moreover, in Fig. 7, we can see that the outage probability of the source user for PS relaying is higher than the TS relaying. Also, we can notice that, for PS relaying at ε = 0.5,& 0.7 is almost same from 0 to 10 dB which means that the choice of power splitting factor ε at transmit SNR less than 10 dB do not have significant role unlike TS relaying where we can clearly see the decrements in outage probability with the increase in α. Moreover, our analysis for TS, PS and NOMA in the presence of interfering signal exactly matched with the simulation results.

Similarly, in Fig. 8, the outage probability of the IoT relay user IoT_R is plotted against the transmit SNR. We can see a similar trend as in Fig. 7 with a clear difference in the outage probability at ε = 0.5,& 0.7. Although at less than 6 dB transmit SNR, the outage probability for IoT_R is shown lower than the source user, the outage probability for IoT_R is shown higher for both TS, PS relaying in the presence of interfering signal at transmit SNR higher than 6 dB which means that the interfering signal has a dominant effect in the outage probability for IoT_R as compared to source user. Moreover, in Fig. 8, the exact expression and analytical approximation (up to 20 terms) for IoT_R exactly matched with the simulation results which validate that our mathematical analysis is correct as stated in Theorem 2.

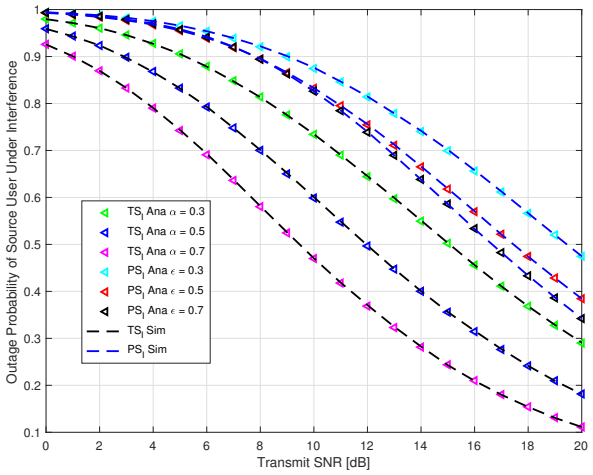

Fig. 7. Outage Probability of Source User with Interfering Signal

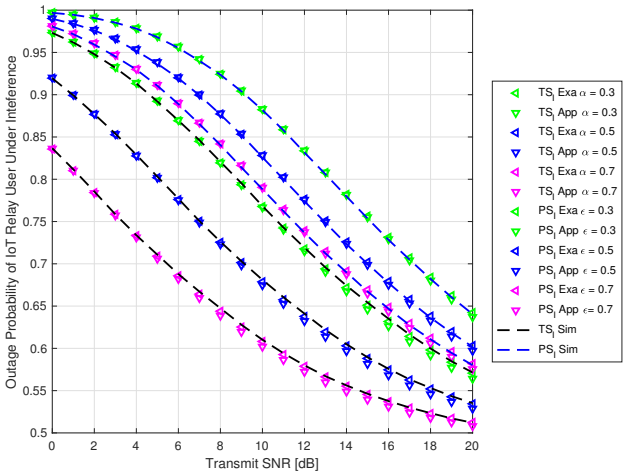

Fig. 8. Outage Probability of IoT Relay User with Interfering Signal

Considering, the source user and the IoT relay user as two user in the system for our consider system model with interfering signal, in Fig. 9, we plotted the sum-throughput against the transmit SNR at different time switching factor α = 0.3, 0.5, & 0.7 and at different power splitting factor ε = 0.3, 0.5, & 0.7. We can see that, for TS relaying, although at α = 0.3, gives the lowest sum-throughput for transmit SNR less than 12 dB as compared to α = 0.5 and α = 0.7, it shows the higher sum-throughput for transmit SNR greater than 12 dB. However, for PS relaying, the sum-throughput clearly increases with the increase in ε and transmit SNR. Hence, we can deduce that the choice of α and interfering

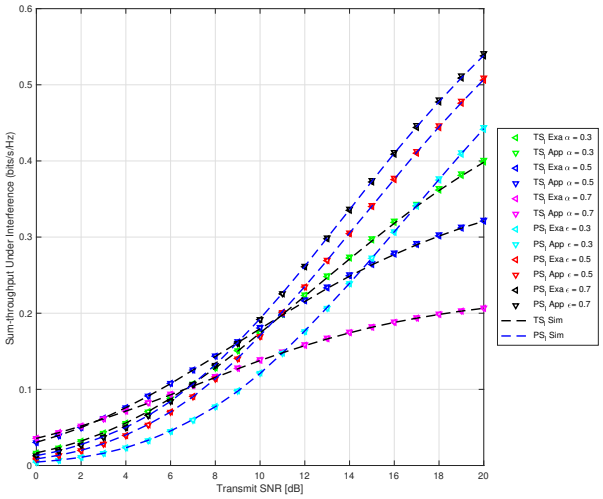

Fig. 9. Sum-throughput of the System with Interfering Signal

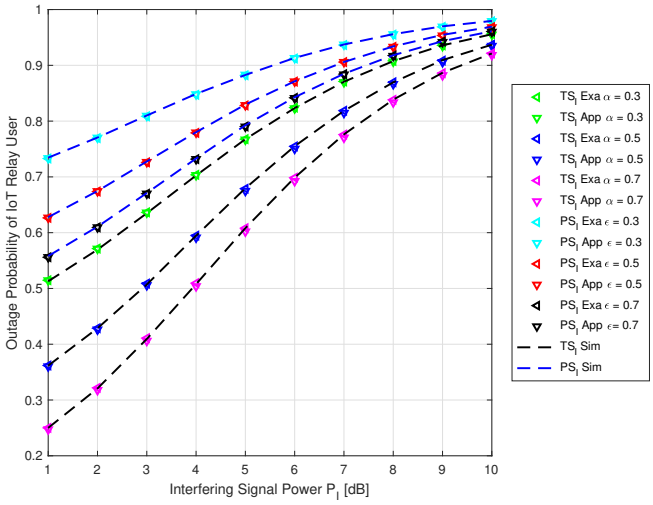

Fig. 11. Outage Probability of IoT Relay User

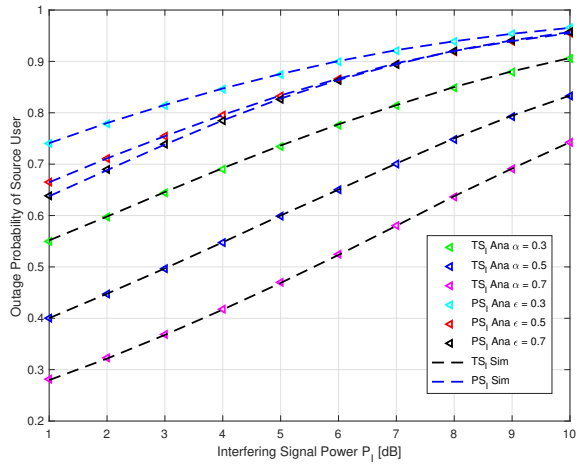

Fig. 10. Outage Probability of Source User

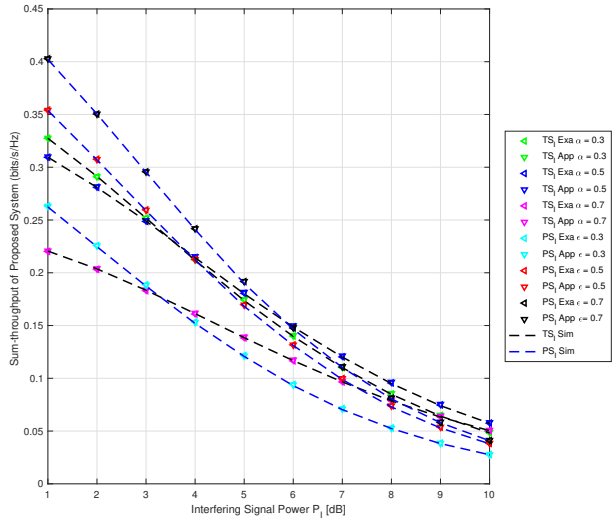

Fig. 12. Sum-throughput of the System

signal greatly affect the sum-throughput for TS relaying than the PS relaying protocol.

Next, we intended to check the performance of system model with varying interfering signal power. So, we plotted the outage probability of the source user and IoT_R for TS and PS relaying against the interfering signal power in Fig. 10 and Fig. 11 respectively at 10 dB transmit SNR, at different α = 0.3, 0.5, & 0.7 and at different ε = 0.3, 0.5, & 0.7. We can see that the outage probability is an increasing function with respect to interfering signal power for both source and IoT_R. Also, the outage probability for PS relaying is shown higher than TS relaying against the same amount of time switching factor α = 0.3, 0.5, & 0.7 and power splitting factor ε = 0.3, 0.5, & 0.7. Also, it can be seen from Fig. 10, for interfering signal power greater than 5 dB, the outage probability of the source user for PS relaying has identical performance at ε = 0.5, & 0.7, which indicates that interfering signal power has a significant role in the outage probability of the source user for PS relaying as compared to TS relaying.

In Fig. 12, we plotted the sum-throughput of the considered system model against the interfering signal power. Although, the sum-throughput is a decreasing function for both TS and PS relaying with respect to interfering signal power, it is interesting to note that the sum-throughput for TS at α = 0.5 shows the higher performance than PS relaying at interfering signal power higher than 6 dB. Also, as seen in Fig. 9 where the sum-throughput for PS is shown higher than TS relaying at higher transmit SNR, it can be seen from Fig. 12 that the interfering signal power has higher effect on the sum-throughput for PS relaying than the TS relaying.

Next, we wanted to verify our analysis for the considered system model with interfering signal against the time switching factor α and power splitting factor ε for both TS and PS relaying protocol. We plotted the sum-throughput

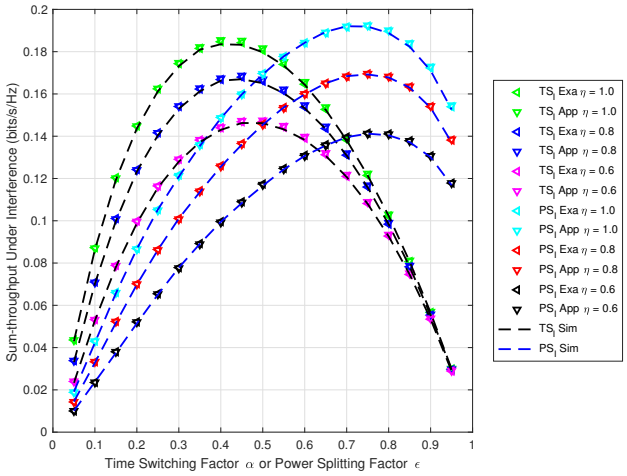

Fig. 13. Sum-throughput of the System v/s α or ε at Different Energy Harvesting Factor

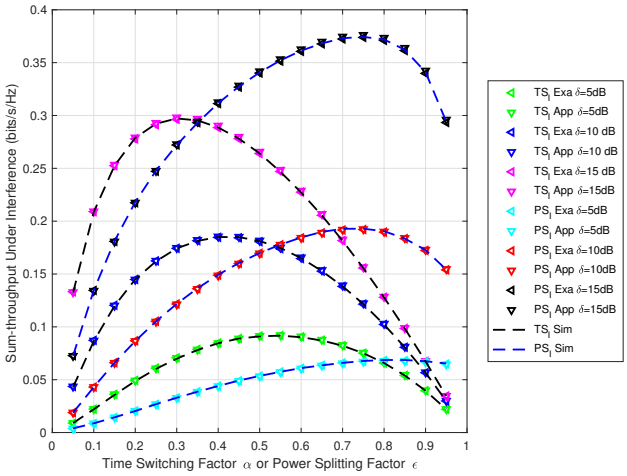

Fig. 14. Sum-throughput of the System v/s α or ε at Different Transmit SNR

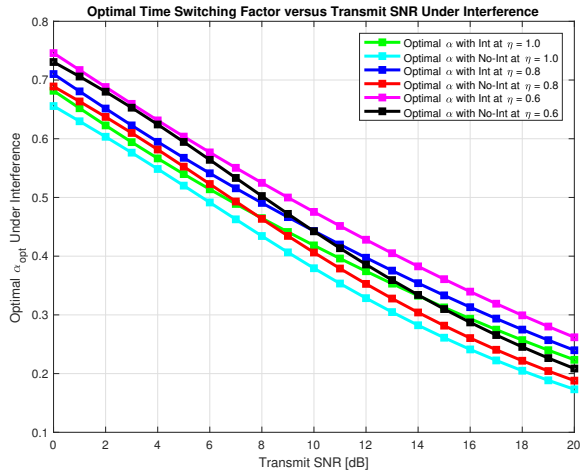

Fig. 15. Optimal α Under Interfering Signal

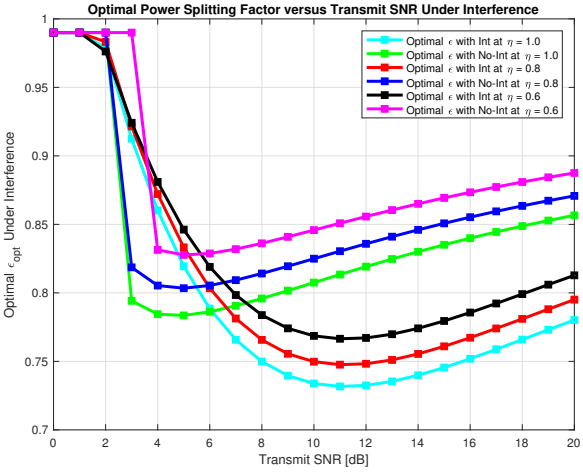

Fig. 16. Optimal ε Under Interfering Signal

against the α and ε varying from 0 to 1 and at η = 0.6, 0.8, & 1.0 and δ = 5 dB, 10 dB, & 15 dB in Fig. 13 and Fig. 14 respectively. For plotting the Fig. 13, the transmit SNR was kept at 10 dB. We can observe in Fig. 13 that the sum-throughput first increases with the increase in η, α and ε, reaches to the maximum and then decreases for both TS and PS relaying. A similar trend can be seen in Fig. 14, the sum-throughput first increases with increase in transmit SNR, α and ε, reaches to the maximum and then decreases for both TS and PS relaying which indicates that the sum-throughput is a concave function which has a unique maxima α^*, ε^* on the interval $[0,1]$ that maximizes the sum-throughput for our system model under consideration in the presence of interfering signal as explained in the Section VI. Therefore, we need to find out the optimal α^*, ε^* that maximizes the sum-throughput.

In Fig. 15, we found out the optimal time switching factor α^* under interference using the iterative numerical method- Golden section search method against the transmit SNR at different energy harvesting factor η = 0.6, 0.8, & 1.0. We can see that optimal α^* linearly decrease with the increase in transmit SNR. For comparison, we also plotted the optimal time switching factor α^* with no interfering signal as denoted by $'No-Int'$ in Fig. 15. Clearly, we can see that, optimal α^* is lower for no interfering signal against all transmit SNR is lower than the optimal α^* with interfering signal which means that the interfering signal power has dominant role in increasing the value of optimal time switching α^*. Moreover, as energy harvesting factor η increases, the optimal α^* for the considered system model with interfering signal and without interfering signal decreases.

Similarly, In Fig. 16, we found out the optimal power splitting ε^* under interference using the iterative numerical method- Golden section search method against transmit SNR at different energy harvesting factor η = 0.6, 0.8, & 1.0. We can see that optimal ε^* first decrease with increase in transmit SNR upto 12 dB then slightly tends to increase. Also, it can be seen from Fig. 16 that the optimal ε^* with

interfering signal at η = 0.6 has lower optimal ε^* than η = 0.8 & 1.0 at transmit SNR less than 3 dB. However, optimal ε^* with interfering signal at η = 0.6 tends to increase than optimal ε^* than η = 0.8 & 1.0 at transmit SNR greater than 3 dB. For comparison, we also plotted the optimal power splitting factor ε^* with no interfering signal as denoted by $'No-Int'$ in Fig. 16. Here, we can see that the optimal ε^* is higher for no interfering signal against all transmit SNR than the optimal ε^* with interfering signal which means that the interfering signal power tends to lower the value of optimal power splitting ε^*. Moreover, as energy harvesting factor η increases, the optimal ε^* for the considered system model with interfering signal and without interfering signal decreases. It is important to find the optimal α^* and ε^* for maximizing the sum-throughput and lowering the possibility of outage in the system.

VIII. Conclusion and Future Works

In this paper, we investigated the performance analysis of RF energy harvesting and information transmission based on NOMA with an interfering signal for IoT relay systems. Different from generic RF EH system in the literature where only a source node data is relayed through intermediate EH relaying node, in this paper, we also considered transmitting the data of IoT relay node along with the source node data using NOMA protocol in the presence of an interfering signal to their respective destinations. Considering our system model with practical interference constraint, we studied TS and PS relaying with NOMA suitable for IoT relay systems. We have mathematically derived the outage probability, throughput and sum-throughput for our considered system model based on TS, PS and NOMA with interfering signal where we verified our derived mathematical analysis (exact and approximation) with the Monte-Carlo simulation results and representative performance comparisons were presented thoroughly. The optimal choice of time switching factor α, power splitting factor ε under the influence of interfering signal affect the system performance greatly. Therefore, through iterative Golden section search method, we found out the optimal time switching factor α^* and optimal power splitting factor ε^* that maximizes the sum-throughput for our considered system model with the interfering signal.

For future work, it would be interesting to use IoT relay user as a bi-directional relay where it can be used to recharge itself and other IoT nodes and transmits the information to the wireless access points or hybrid access points under Quality-of-Service (QoS) constraints. It would also be interesting to apply game theory approach for power allocation for RF EH under the influence of various interfering signals. Also, investigating the secrecy capacity for secured communication in IoT relay systems is an interesting topic for our future work.

Acknowledgement

The authors would like to gratefully acknowledge the anonymous reviewers for their thoughtful and detailed comments which helped in improving the quality of this paper.

Appendix A
Proof of Theorem 1

From Equation. 14, we have,

$$P_{IOut_S} = Pr(min(\gamma_{IIoT_R}, \gamma_{Is_{rec}}) < \psi)$$
$$= 1 - Pr(min(\gamma_{IIoT_R}, \gamma_{Is_{rec}}) \geq \psi)$$
$$= 1 - Pr(\frac{\delta X}{P_I F_1} \geq \psi, \frac{\phi_1 P_{IoT_R} Y}{P_I F_2} \geq \psi)$$
$$= 1 - Pr(\frac{\delta X}{P_I F_1} \geq \psi, \frac{\phi_1 2\eta P_s X \alpha Y}{(1-\alpha) P_I F_2} \geq \psi)$$

Put $a = \frac{\delta}{P_I}$ and $b = \frac{2\eta\phi_1 P_s \alpha}{(1-\alpha)P_I}$

$$= 1 - Pr(\frac{aX}{F_1} \geq \psi, \frac{bXY}{F_2} \geq \psi)$$
$$= 1 - Pr(F_1 \leq \frac{aX}{\psi}, Y \geq \frac{\psi F_2}{bX})$$

Conditioning on X, we have

$$= 1 - \int_0^\infty \underbrace{Pr\big(F_1 \leq \frac{aX}{\psi} | X = x\big)}_{I_1} \times \underbrace{Pr\big(Y \geq \frac{\psi F_2}{bX} | X = x\big)}_{I_2} f_X(x) dx$$

Let us evaluate I_1,

$$I_1 = \int_0^{\frac{ax}{\psi}} \lambda_{f_1} e^{-\lambda_{f_1} f_1} df_1$$
$$= 1 - e^{\frac{-\lambda_{f_1} ax}{\psi}}$$

Let us evaluate I_2,

$$I_2 = Pr\big(Y \geq \frac{\psi F_2}{bX} | X = x\big)$$
$$= Pr\big(Y \geq \frac{\psi F_2}{bx}\big)$$

Now, again conditioning I_2 on F_2, we get,

$$I_2 = \int_0^\infty Pr\big(Y \geq \frac{\psi f_2}{bx}\big) f_{F_2}(f_2) df_2$$
$$= \int_0^\infty \big(\int_{\frac{\psi f_2}{bx}}^\infty \lambda_g e^{-\lambda_g y} dy\big) \lambda_{f_2} e^{-\lambda_{f_2} f_2} df_2$$
$$= \int_0^\infty e^{-\frac{\lambda_g \psi f_2}{bx}} \lambda_{f_2} e^{-\lambda_{f_2} f_2} df_2$$
$$= \frac{\lambda_{f_2}}{\frac{\lambda_g \psi}{bx} + \lambda_{f_2}}$$

Now,

$$= 1 - \int_0^\infty I_1 . I_2 . \lambda_h e^{-\lambda_h x} dx$$
$$= 1 - \lambda_h \int_0^\infty \big(1 - e^{\frac{-\lambda_{f_1} ax}{\psi}}\big)\big(\frac{\lambda_{f_2}}{\frac{\lambda_g \psi}{bx} + \lambda_{f_2}}\big) e^{-\lambda_h x} dx$$

Multiplying Numerator and Denominator by $\frac{x}{\lambda_{f_2}}$

$$= 1 - \lambda_h \int_0^\infty \frac{x}{m+x}(1 - e^{-nx}) e^{-\lambda_h x} dx$$

where $m = \frac{\lambda_g \psi}{\lambda_{f_2} b}$ and $n = \frac{\lambda_{f_1} a}{\psi}$

From, [37], Equation 3.353.5, we know that,

$$\int_0^\infty \frac{x}{x+\beta}e^{-ux} = \beta e^{u\beta}Ei(-u\beta)+\frac{1}{u}$$
$$= 1-\lambda_h\left(\int_0^\infty \frac{x}{m+x}e^{-\lambda_h x}dx - \int_0^\infty \frac{x}{m+x}e^{-n-\lambda_h x}dx\right)$$
$$= 1-\lambda_h\left(\left(me^{\lambda_h m}Ei\big(-m\lambda_h\big)+\frac{1}{\lambda_h}\right)-\right.$$
$$\left.\left(me^{(n+\lambda_h)m}Ei\big(-(n+\lambda_h)m\big)+\frac{1}{(n+\lambda_h)}\right)\right)$$
$$= 1-\lambda_h me^{\lambda_h m}Ei\big(-m\lambda_h\big)-1+$$
$$\lambda_h me^{(n+\lambda_h)m}Ei\big(-(n+\lambda_h)m\big)+\frac{\lambda_h}{(n+\lambda_h)}$$
Since, $Ei(x) = -Ei(-x)$
$$= \lambda_h me^{\lambda_h m}Ei\big(m\lambda_h\big)-\lambda_h me^{(n+\lambda_h)m}Ei\big((n+\lambda_h)m\big)+$$
$$\frac{\lambda_h}{(n+\lambda_h)}$$
Therefore,
$$P_{IOut_S} = \lambda_h me^{\lambda_h m}Ei\big(m\lambda_h\big)-\lambda_h me^{(n+\lambda_h)m}Ei\big((n+\lambda_h)m\big)$$
$$+\frac{\lambda_h}{(n+\lambda_h)}$$
Putting the value of P_{IOut_S} in Equation. 16, we get,
$$Thr_{IS} = \frac{(1-\alpha)R}{2}\left(1-\lambda_h me^{\lambda_h m}Ei\big(m\lambda_h\big)\right.$$
$$\left.+\lambda_h me^{(n+\lambda_h)m}Ei\big((n+\lambda_h)m\big)-\frac{\lambda_h}{(n+\lambda_h)}\right)$$
This ends the proof of Theorem 1.

APPENDIX B
PROOF OF THEOREM 2

From Equation. 16, we have,
$$P_{IOut_{IoT_R}} = Pr(min(\gamma_{I_{S_{rec}}}^{x_{IoT_R}\to x_s}, \gamma_{IIoT_{rec}}) \le \psi)$$
$$= 1-Pr(min(\gamma_{I_{S_{rec}}}^{x_{IoT_R}\to x_s}, \gamma_{IIoT_{rec}}) \ge \psi)$$
$$= 1-$$
$$Pr\left(\frac{\phi_2 P_{IoT_R}Y}{\phi_1 P_{IoT_R}YP_IF_2+1}\ge\psi, \frac{\phi_2 P_{IoT_R}Z}{\phi_1 P_{IoT_R}ZP_IF_3+1}\ge\psi\right)$$
$$= 1-$$
$$Pr\left(\frac{\phi_2\frac{2\eta P_sX\alpha}{(1-\alpha)}Y}{\phi_1\frac{2\eta P_sX\alpha}{(1-\alpha)}YP_IF_2+1}\ge\psi, \frac{\phi_2\frac{2\eta P_sX\alpha}{(1-\alpha)}Z}{\phi_1\frac{2\eta P_sX\alpha}{(1-\alpha)}ZP_IF_3+1}\ge\psi\right)$$
Put $l = \frac{2\eta P_s\alpha}{(1-\alpha)}$, and $t = \frac{2\eta P_s\alpha P_I}{(1-\alpha)}$
$$= 1-Pr\left(\frac{\phi_2 XYl}{\phi_1 XYF_2t+1}\ge\psi, \frac{\phi_2 XZl}{\phi_1 XZF_3t+1}\ge\psi\right)$$
$$= 1-Pr\left(Y\ge\frac{\psi}{(\phi_2 l-\phi_1 tF_2\psi)X}, Z\ge\frac{\psi}{(\phi_2 l-\phi_1 tF_3\psi)X}\right)$$
Conditioning on X,
$$= 1-\int_0^\infty Pr\big(Y\ge\frac{\psi}{(\phi_2 l-\phi_1 tF_2\psi)X}|X=x\big)\times$$
$$Pr\big(Z\ge\frac{\psi}{(\phi_2 l-\phi_1 tF_3\psi)X}|X=x\big)f_X(x)dx$$
$$= 1-\int_0^\infty Pr\big(Y\ge\frac{\psi}{(\phi_2 l-\phi_1 tF_2\psi)x}\big)Pr\big(Z\ge\frac{\psi}{(\phi_2 l-\phi_1 tF_3\psi)x}\big)\times$$
$$\lambda_h e^{-\lambda_h x}dx$$
$$= 1-\lambda_h\int_0^\infty e^{-\left(\frac{4\lambda_g\psi}{(\phi_2 l-\phi_1 tF_2\psi)}+\frac{4\lambda_z\psi}{(\phi_2 l-\phi_1 tF_3\psi)}\right)\frac{1}{4x}-\lambda_h x}dx$$
Now, by using the formula,
$$\int_0^\infty e^{-\frac{\beta}{4x}-\gamma x}dx = \sqrt{\frac{\beta}{\gamma}}K_1\big(\sqrt{\beta\gamma}\big)[37], \text{Eq. } 3.324.1$$
$$= 1-2\sqrt{\frac{\lambda_h\lambda_g\psi}{\phi_2 l-\phi_1 tF_2\psi}+\frac{\lambda_h\lambda_z\psi}{\phi_2 l-\phi_1 tF_3\psi}}\times$$
$$K_1\left(2\sqrt{\frac{\lambda_h\lambda_g\psi}{\phi_2 l-\phi_1 tF_2\psi}+\frac{\lambda_h\lambda_z\psi}{\phi_2 l-\phi_1 tF_3\psi}}\right)$$
Now, conditioning on F_2
$$= 1-\int_0^{\frac{\phi_2 l}{\phi_1 t\psi}} 2\sqrt{\frac{\lambda_h\lambda_g\psi}{\phi_2 l-\phi_1 tf_2\psi}+\frac{\lambda_h\lambda_z\psi}{\phi_2 l-\phi_1 tF_3\psi}}\times$$
$$K_1\left(2\sqrt{\frac{\lambda_h\lambda_g\psi}{\phi_2 l-\phi_1 tf_2\psi}+\frac{\lambda_h\lambda_z\psi}{\phi_2 l-\phi_1 tF_3\psi}}\right)\lambda_{f_2}e^{-\lambda_{f_2}f_2}df_2$$
Again, conditioning on F_3
$$= 1-\lambda_{f_2}\lambda_{f_3}\int_0^{\frac{\phi_2 l}{\phi_1 t\psi}}\int_0^{\frac{\phi_2 l}{\phi_1 t\psi}} 2\sqrt{\frac{\lambda_h\lambda_g\psi}{\phi_2 l-\phi_1 tf_2\psi}+\frac{\lambda_h\lambda_z\psi}{\phi_2 l-\phi_1 tf_3\psi}}\times$$
$$K_1\left(2\sqrt{\frac{\lambda_h\lambda_g\psi}{\phi_2 l-\phi_1 tf_2\psi}+\frac{\lambda_h\lambda_z\psi}{\phi_2 l-\phi_1 tf_3\psi}}\right)e^{-\lambda_{f_2}f_2}e^{-\lambda_{f_3}f_3}df_2df_3$$
The above expression is the exact expression for outage probability $P_{Exact-IOut_{IoT_R}}$ as shown in Equation. 23
Now, putting the value of $P_{Exact-IOut_{IoT_R}}$ in Equation. 17 we get the exact equation for throughput $Thr_{Exact-IIoT_R}$ as shown in Equation. 24
Now, let, $u = \frac{\lambda_h\lambda_g\psi}{\phi_2 l-\phi_1 tf_2\psi}$ and $v = \frac{\lambda_h\lambda_z\psi}{\phi_2 l-\phi_1 tf_3\psi}$
Then, $f_2 = \frac{\phi_2 l}{\phi_1 t\psi}-\frac{\lambda_h\lambda_g}{\phi_1 tu} \to df_2 = \frac{\lambda_h\lambda_g}{\phi_1 tu^2}du$
Similarly, $f_3 = \frac{\phi_2 l}{\phi_1 t\psi}-\frac{\lambda_h\lambda_z}{\phi_1 tv} \to df_3 = \frac{\lambda_h\lambda_z}{\phi_1 tv^2}dv$
$$P_{IOut_{IoT_R}} = 1-\frac{\lambda_{f_2}\lambda_{f_3}\lambda_h^2\lambda_g\lambda_z}{(\phi_1 t)^2}e^{-(\lambda_{f_2}+\lambda_{f_3})\frac{\phi_2 l}{\phi_1 t\psi}}\times$$
$$\int_{u=\frac{\lambda_h\lambda_g\psi}{\phi_2 l}}^\infty\int_{v=\frac{\lambda_h\lambda_z\psi}{\phi_2 l}}^\infty\frac{2}{u^2v^2}\sqrt{u+v}K_1(2\sqrt{u+v})e^{\frac{\lambda_{f_2}\lambda_h\lambda_g}{\phi_1 tm}+\frac{\lambda_{f_3}\lambda_h\lambda_z}{\phi_1 tn}}dudv$$
Let, $a_2 = \frac{\lambda_{f_2}\lambda_h\lambda_g}{\phi_1 t}, a_3 = \frac{\lambda_{f_3}\lambda_h\lambda_z}{\phi_1 t}, b_2 = \frac{\lambda_h\lambda_g}{\phi_2 l}, b_3 = \frac{\lambda_h\lambda_z}{\phi_2 l}$
$$P_{IOut_{IoT_R}} = 1-a_2a_3e^{-\left(\frac{a_2}{b_2}+\frac{a_3}{b_3}\right)\frac{1}{\psi}}\times$$
$$\int_{u=b_2\psi}^\infty\int_{v=b_3\psi}^\infty\frac{1}{u^2v^2}e^{\frac{a_2}{u}+\frac{a_3}{v}}H(u+v)dudv$$

where $H(z) = 2\sqrt{(z)}K_1(2\sqrt{(z)})$

Again changing the integration variables as,

$x = 1 - \frac{b_2\psi}{u}$ and $y = 1 - \frac{b_3\psi}{v}$, we get,

$$P_{IOut_{IoT_R}} = 1 - \frac{a_2}{b_2\psi}\frac{a_3}{b_3\psi}\int_{x=0}^{1}\int_{y=0}^{1} e^{-(\frac{a_2 x}{b_2\psi}+\frac{a_3 y}{b_3\psi})} \times H\left(\frac{b_2\psi}{1-x}+\frac{b_3\psi}{1-y}\right)dxdy$$

Now, expanding $H\left(\frac{b_2\psi}{1-x}+\frac{b_3\psi}{1-y}\right)$ in two dimensional power series and integrating term by term, we get,

$$H\left(\frac{b_2\psi}{1-x}+\frac{b_3\psi}{1-y}\right) = \sum_{k=0}^{\infty}\frac{1}{k!}H^{(k)}(b_2\psi+b_3\psi)\times \left(b_2\psi\frac{x}{1-x}+b_3\psi\frac{y}{1-y}\right)^k$$

where, nth derivative, $H^{(n)}(z) = (-1)^n 2(\sqrt{z})^{1-n}K_{n-1}(2\sqrt{z})$

By using Binomial Formula,

$$= \sum_{k=0}^{\infty}\frac{1}{k!}H^{(k)}(b_2\psi+b_3\psi)\sum_{l=0}^{k}\binom{k}{l}(b_2\psi)^l(b_3\psi)^{k-l}\times x^l(1-x)^{-l}y^{k-l}(1-y)^{-k+l}$$

Changing the summation order, the above expression can be rewritten as,

$$\sum_{l=0}^{\infty}\sum_{k=0}^{\infty}\frac{1}{k!\,l!}H^{(k+l)}(b_2\psi+b_3\psi)(b_2\psi)^l(b_3\psi)^k x^l(1-x)^{-l}y^k(1-y)^{-k}$$

Now,

$$(1-x)^{-l} = \sum_{s=0}^{\infty}(-1)^s\binom{-l}{s}x^s = \sum_{s=0}^{\infty}\binom{l+s-1}{l-1}x^s$$

$$(1-y)^{-k} = \sum_{n=0}^{\infty}(-1)^n\binom{-k}{n}y^n = \sum_{n=0}^{\infty}\binom{k+n-1}{k-1}y^n$$

$$= \sum_{l=0}^{\infty}\sum_{k=0}^{\infty}\sum_{s=0}^{\infty}\sum_{n=0}^{\infty}\frac{1}{k!\,l!}\binom{l+s-1}{l-1}\binom{k+n-1}{k-1}H^{(k+l)}(b_2\psi+b_3\psi)\times (b_2\psi)^l(b_3\psi)^k x^{l+s}y^{k+n}$$

Summing by taking $i = l+s$ and $j = k+n$,

$$= \sum_{i=0}^{\infty}\sum_{j=0}^{\infty}\left(\sum_{l=0}^{i}\sum_{k=0}^{j}\frac{1}{k!\,l!}\binom{i-1}{l-1}\binom{j-1}{k-1}H^{(k+l)}(b_2\psi+b_3\psi)\times (b_2\psi)^l(b_3\psi)^k\right)x^i y^j$$

Therefore, $H\left(\frac{b_2\psi}{1-x}+\frac{b_3\psi}{1-y}\right) = \sum_{i=0}^{\infty}\sum_{j=0}^{\infty}C_{ij}x^i y^j$

where,

$$C_{ij} = \sum_{l=0}^{i}\sum_{k=0}^{j}\frac{1}{k!\,l!}\binom{i-1}{l-1}\binom{j-1}{k-1}H^{(k+l)}(b_2\psi+b_3\psi)(b_2\psi)^l(b_3\psi)^k$$

Now, integrating term by term we find,

$$P_{IOut_{IoT_R}} = 1 - \sum_{i=0}^{\infty}\sum_{j=0}^{\infty}C_{ij}\frac{a_2}{b_2\psi}\frac{a_3}{b_3\psi}\int_{x=0}^{1}\int_{y=0}^{1}e^{-(\frac{a_2 x}{b_2\psi}+\frac{a_3 y}{b_3\psi})}x^i y^j dxdy$$

$$= 1 - \sum_{i=0}^{\infty}\sum_{j=0}^{\infty}C_{ij}I\left(i,\frac{a_2}{b_2\psi}\right)I\left(j,\frac{a_3}{b_3\psi}\right)$$

where,

$I(k,a) = a\int_{x=0}^{1}x^k e^{-ax}dx = k!\,a^{-k}\left(1 - S_k(a)e^{-a}\right)$ and

$S_k(a) = \sum_{s=0}^{k}\frac{a^s}{s!}$ is truncated exponential series

Hence,

$$P_{IOut_{IoT_R}} = 1 - \sum_{i=0}^{\infty}\sum_{j=0}^{\infty}i!\,j!\,C_{ij}\left(\frac{b_2\psi}{a_2}\right)^i\left(\frac{b_3\psi}{a_3}\right)^j\times \left(1 - S_i(\frac{a_2}{b_2\psi})e^{-\frac{a_2}{b_2\psi}}\right)\left(1 - S_j(\frac{a_3}{b_3\psi})e^{-\frac{a_3}{b_3\psi}}\right)$$

Putting the value of $P_{IOut_{IoT_R}}$ in Equation. 17, we get,

$$Thr_{IIoT_R} = \frac{(1-\alpha)R}{2}\sum_{i=0}^{\infty}\sum_{j=0}^{\infty}i!\,j!\,C_{ij}\left(\frac{b_2\psi}{a_2}\right)^i\left(\frac{b_3\psi}{a_3}\right)^j\times \left(1 - S_i(\frac{a_2}{b_2\psi})e^{-\frac{a_2}{b_2\psi}}\right)\left(1 - S_j(\frac{a_3}{b_3\psi})e^{-\frac{a_3}{b_3\psi}}\right)$$

This ends the proof of Theorem 2.

REFERENCES

[1] D. Evans, "The internet of things: How the next evolution of the internet is changing everything. 2011," *URL http://www. cisco. com/web/about/ac79/docs/innov/IoT IBSG 0411FINAL. pdf*, 2015.

[2] M. R. Palattella, M. Dohler, A. Grieco, G. Rizzo, J. Torsner, T. Engel, and L. Ladid, "Internet of things in the 5g era: Enablers, architecture, and business models," *IEEE Journal on Selected Areas in Communications*, vol. 34, no. 3, pp. 510–527, 2016.

[3] H. Shariatmadari, R. Ratasuk, S. Iraji, A. Laya, T. Taleb, R. Jäntti, and A. Ghosh, "Machine-type communications: current status and future perspectives toward 5g systems," *IEEE Communications Magazine*, vol. 53, no. 9, pp. 10–17, 2015.

[4] S. D. T. Kelly, N. K. Suryadevara, and S. C. Mukhopadhyay, "Towards the implementation of iot for environmental condition monitoring in homes," *IEEE Sensors Journal*, vol. 13, no. 10, pp. 3846–3853, Oct 2013.

[5] A. Rauniyar, D. H. Hagos, and M. Shrestha, "A crowd-based intelligence approach for measurable security, privacy, and dependability in internet of automated vehicles with vehicular fog," *Mobile Information Systems*, vol. 2018, 2018.

[6] M. Wollschlaeger, T. Sauter, and J. Jasperneite, "The future of industrial communication: Automation networks in the era of the internet of things and industry 4.0," *IEEE Industrial Electronics Magazine*, vol. 11, no. 1, pp. 17–27, March 2017.

[7] L. Guntupalli, M. Gidlund, and F. Y. Li, "An on-demand energy requesting scheme for wireless energy harvesting powered iot networks," *IEEE Internet of Things Journal*, vol. 5, no. 4, pp. 2868–2879, Aug 2018.

[8] B. Vejlgaard, M. Lauridsen, H. Nguyen, I. Z. Kovács, P. Mogensen, and M. Sorensen, "Interference impact on coverage and capacity for low power wide area iot networks," in *Wireless Communications and Networking Conference (WCNC), 2017 IEEE*. IEEE, 2017, pp. 1–6.

[9] X. Liang, M. Chen, I. Balasingham, and V. C. Leung, "Cooperative communications with relay selection for wireless networks: design issues and applications," *Wireless Communications and Mobile Computing*, vol. 13, no. 8, pp. 745–759, 2013.

[10] B. Razeghi, G. A. Hodtani, and T. Nikazad, "Multiple criteria relay selection scheme in cooperative communication networks," *Wireless Personal Communications*, vol. 96, no. 2, pp. 2539–2561, 2017.

[11] A. S. Ibrahim, A. K. Sadek, W. Su, and K. R. Liu, "Cooperative communications with relay-selection: when to cooperate and whom to cooperate with?" *IEEE Transactions on Wireless Communications*, vol. 7, no. 7, 2008.

[12] K. Geng, Q. Gao, L. Fei, and H. Xiong, "Relay selection in cooperative communication systems over continuous time-varying fading channel," *Chinese Journal of Aeronautics*, vol. 30, no. 1, pp. 391–398, 2017.

[13] X. Lu, P. Wang, D. Niyato, D. I. Kim, and Z. Han, "Wireless networks with rf energy harvesting: A contemporary survey," *IEEE Communications Surveys & Tutorials*, vol. 17, no. 2, pp. 757–789, 2015.

[14] H. J. Visser and R. J. Vullers, "Rf energy harvesting and transport for wireless sensor network applications: Principles and requirements," *Proceedings of the IEEE*, vol. 101, no. 6, pp. 1410–1423, 2013.
[15] W. Guo, S. Zhou, Y. Chen, S. Wang, X. Chu, and Z. Niu, "Simultaneous information and energy flow for iot relay systems with crowd harvesting," *IEEE Communications Magazine*, vol. 54, no. 11, pp. 143–149, November 2016.
[16] J.-H. Lee, W.-J. Jung, J.-W. Jung, J.-E. Jang, and J.-S. Park, "A matched rf charger for wireless rf power harvesting system," *Microwave and Optical Technology Letters*, vol. 57, no. 7, pp. 1622–1625, 2015.
[17] R. Ge, H. Pan, Z. Lin, N. Gong, J. Wang, and X. Chen, "Rf-powered battery-less wireless sensor network in structural monitoring," in *2016 IEEE international conference on electro information technology (EIT)*. IEEE, 2016, pp. 0547–0552.
[18] L.-G. Tran, H.-K. Cha, and W.-T. Park, "Rf power harvesting: a review on designing methodologies and applications," *Micro and Nano Systems Letters*, vol. 5, no. 1, p. 14, 2017.
[19] Z. Behdad, M. Mahdavi, and N. Razmi, "A new relay policy in rf energy harvesting for iot networks-a cooperative network approach," *IEEE Internet of Things Journal*, vol. 5, no. 4, pp. 2715–2728, Aug 2018.
[20] X. Zhou, R. Zhang, and C. K. Ho, "Wireless information and power transfer: Architecture design and rate-energy tradeoff," *IEEE Transactions on Communications*, vol. 61, no. 11, pp. 4754–4767, November 2013.
[21] R. Zhang and C. K. Ho, "Mimo broadcasting for simultaneous wireless information and power transfer," *IEEE Transactions on Wireless Communications*, vol. 12, no. 5, pp. 1989–2001, 2013.
[22] V. W. Wong, R. Schober, D. W. K. Ng, and L.-C. Wang, *Key technologies for 5G wireless systems*. Cambridge university press, 2017.
[23] Z. Ding, X. Lei, G. K. Karagiannidis, R. Schober, J. Yuan, and V. K. Bhargava, "A survey on non-orthogonal multiple access for 5g networks: Research challenges and future trends," *IEEE Journal on Selected Areas in Communications*, vol. 35, no. 10, pp. 2181–2195, Oct 2017.
[24] L. Dai, B. Wang, Y. Yuan, S. Han, I. Chih-Lin, and Z. Wang, "Non-orthogonal multiple access for 5g: solutions, challenges, opportunities, and future research trends," *IEEE Communications Magazine*, vol. 53, no. 9, pp. 74–81, 2015.
[25] Z. Ding, Z. Yang, P. Fan, and H. V. Poor, "On the performance of non-orthogonal multiple access in 5g systems with randomly deployed users," *arXiv preprint arXiv:1406.1516*, 2014.
[26] Y. Saito, Y. Kishiyama, A. Benjebbour, T. Nakamura, A. Li, and K. Higuchi, "Non-orthogonal multiple access (noma) for cellular future radio access," in *2013 IEEE 77th Vehicular Technology Conference (VTC Spring)*. IEEE, 2013, pp. 1–5.
[27] A. A. Nasir, X. Zhou, S. Durrani, and R. A. Kennedy, "Wireless-powered relays in cooperative communications: Time-switching relaying protocols and throughput analysis," *IEEE Transactions on Communications*, vol. 63, no. 5, pp. 1607–1622, 2015.
[28] Y. Gu and S. Aissa, "Rf-based energy harvesting in decode-and-forward relaying systems: Ergodic and outage capacities," *IEEE Transactions on Wireless Communications*, vol. 14, no. 11, pp. 6425–6434, 2015.
[29] L. Elmorshedy, C. Leung, and S. A. Mousavifar, "Rf energy harvesting in df relay networks in the presence of an interfering signal," in *2016 IEEE International Conference on Communications (ICC)*. IEEE, 2016, pp. 1–6.
[30] D.-T. Do and H.-S. Nguyen, "A tractable approach to analyzing the energy-aware two-way relaying networks in the presence of co-channel interference," *EURASIP Journal on Wireless Communications and Networking*, vol. 2016, no. 1, p. 271, 2016.
[31] D.-T. Do and C.-B. Le, "Application of noma in wireless system with wireless power transfer scheme: Outage and ergodic capacity performance analysis," *Sensors*, vol. 18, no. 10, p. 3501, 2018.
[32] A. Rauniyar, P. Engelstad, and O. Østerbø, "Rf energy harvesting and information transmission based on noma for wireless powered iot relay systems," *Sensors*, vol. 18, no. 10, p. 3254, 2018.
[33] A. D. Wyner, "The wire-tap channel," *Bell system technical journal*, vol. 54, no. 8, pp. 1355–1387, 1975.
[34] B. Sklar, "Rayleigh fading channels in mobile digital communication systems .i. characterization," *IEEE Communications Magazine*, vol. 35, no. 7, pp. 90–100, July 1997.
[35] Z. Yang, Z. Ding, P. Fan, and N. Al-Dhahir, "The impact of power allocation on cooperative non-orthogonal multiple access networks with swipt," *IEEE Transactions on Wireless Communications*, vol. 16, no. 7, pp. 4332–4343, 2017.
[36] M. F. Kader, M. B. Shahab, and S. Y. Shin, "Cooperative spectrum sharing with energy harvesting best secondary user selection and non-orthogonal multiple access," in *2017 International Conference on Computing, Networking and Communications (ICNC)*. IEEE, 2017, pp. 46–51.
[37] I. S. Gradshteyn and I. M. Ryzhik, *Table of integrals, series, and products*. Academic press, 1980.

ASHISH RAUNIYAR is currently working as a PhD Research Fellow with the Autonomous Systems and Sensor Technologies Research Group, Department of Technology Systems, Faculty of Mathematics and Natural Sciences, University of Oslo and Autonomous Systems and Networks (ASN) Research Group, Department of Computer Science, Oslo Metropolitan University, Norway. He was a graduate research assistant at Wireless Emerging Networking System (WENS) Lab, where he completed his Master degree in IT Convergence Engineering at Kumoh National Institute of Technology, South-Korea. He is a recipient of Best Paper Award at IEEE 28th ITNAC Conference, 2018, Sydney, Australia. His main research area includes Internet of Things, Machine Learning, Wireless Communications and Computer Networking.

PAAL E. ENGELSTAD received the Bachelor Degree in Physics from the Norwegian University of Science and Technology (NTNU) in 1993,the Master Degree (Hons.) in Physics from NTNU/Kyoto University, Japan, in 1994, the Ph.D. Degree in Computer Science from the University of Oslo in 2005. He is currently a Full Professor with Oslo Metropolitan University. He is also a Research Scientist at Norwegian Defence Research Establishment and a Professor with the Autonomous Systems and Sensor Technologies Research Group, Department of Technology Systems, University of Oslo. He holds a number of patents and has been publishing a number of papers over the past years. His current research interests include fixed, wireless and adhoc networking, cybersecurity, machine learning, and distributed and autonomous systems.

OLAV N. ØSTERBØ received his M.Sc. in Applied Mathematics from the University of Bergen in 1980 and his Ph.D. from NTNU in 2004. He joined Telenor in 1980 and has more than 30 years of experience in telecom research. Activities in recent years have been related to QoS and performance analysis. Current research topics include traffic modeling, analysis of interference in radio networks, scheduling, traffic differentiation, and M2M.